Design of an Integrated Modular Motor Drive System

Mesut Uğur
Department of Electrical and Electronics Engineering
Middle East Technical University
Ankara, Turkey
ugurm@metu.edu.tr

Ozan Keysan
Department of Electrical and Electronics Engineering
Middle East Technical University
Ankara, Turkey
keysan@metu.edu.tr

Abstract— **In this study, design procedure of an Integrated Modular Motor Drive (IMMD) is presented. The design is based on a modular fractional slot concentrated winding, permanent magnet synchronous machine (FSCW-PMSM) and power stage with gallium nitride (GaN) power field effect transistors (FETs). Suitable slot/pole combination and winding configuration are discussed in order to maximize the stator winding factor as well as to reduce the space harmonics on the modular motor. Optimum selection of number of series and parallel motor drive modules is achieved and power device selection is performed based on loss characterization. Selection of DC link capacitor bank is performed and the effect of interleaving on the capacitor size is investigated. The performance of the system is obtained with ANSYS/Maxwell for the motor and with MATLAB/Simulink for the power stage. The efficiency of the motor drive is enhanced by 2% compared to a conventional motor drive power stage. Power density values as high as 15 W/cm^3 has been achieved which is usually not obtained with conventional motor drive systems.**

Keywords—integrated modular motor drive; permanent magnet synchronous motor; gallium nitride; DC bus capacitor bank

I. INTRODUCTION

In conventional motor drive systems, the drive units are placed in separate cabinets which increases the overall weight and volume of the system and decreases the power density of the system. Furthermore, the drive units are connected to the motor by means of long cables which causes transient voltage overshoots due to the high frequency pulse width modulation (PWM) operation.

A novel concept called Integrated Modular Motor Drives (IMMDs) has been proposed in the last few years suggesting that all the components of the motor drive system can be integrated onto the motor including power electronics, control electronics, passive components and heat sink [1]. By doing so, the power density of the system can be enhanced significantly which is very critical in aerospace and electric traction applications [2]. In addition to that, cost reduction up to 20% is possible thanks to the elimination of enclosures and connection equipment [1]. The absence of connection cables yields less leakage current on the winding insulation which will extend the lifespan of the motor as well as minimize electromagnetic interference (EMI) problems [3].

With modularization, the overall system is segmented with modules sharing the total power equally. By this way, the fault tolerance of the system is increased [4]. The current and voltage ratings of the power semiconductor devices can also be decreased by modularization. Moreover, the components which produce heat due to power loss are spread and distributed in a wider surface area which makes the thermal design more convenient as well as decreases the possible of hot spot formation. Finally, the manufacturing, installation and maintenance costs decrease thanks to the modular structure [1].

However, integration of the motor and drive brings several challenges. First, fitting all the drive components to the available space requires size optimization and careful layout design [3]. Second, it is difficult to cool the motor and drive simultaneously since they both produce heat. Furthermore, all the electronic components are subjected to a higher ambient temperature and continuous vibration and should be selected accordingly [3].

To overcome these challenges, it has been proposed in the literature that wide band gap (WBG) power semiconductor devices such as Gallium Nitride (GaN) can be used which are capable of operating at high frequencies [3]. By doing so, the size of the passive components can be reduced as well as the size of the heat sink thanks to superior efficiency values [5]. However, high frequency operation highlights the parasitic components on the power stage and gate drive circuits which makes layout design critical.

In this paper, design of an IMMD system is presented with enhanced power density, increased efficiency and enhanced fault tolerance capability. In Section 2, basic structure and current technology prospects of IMMDs are introduced. In section 3, design of the system including the motor and the drive is explained. In section 4, simulation results are presented and in section 5, conclusions are given.

II. BASIC STRUCTURE OF IMMD

There are several types of integration of the motor drive onto the motor. In this paper, integration into the stator back iron is considered, which also allows the modularization of the system. In this configuration, one module is composed of a stator pole piece, a concentrated coil and a power converter dedicated to its own winding along with its controller. Examples of such a structure can be seen in Fig. 1 [1].

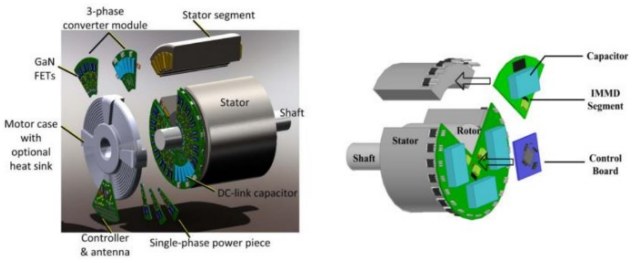

Fig. 1. IMMDs with stator back-iron integration [1]

Each stator winding belonging to different pole pairs on the stator are usually connected in series to form one phase of the stator in conventional motors. On the other hand, the windings in different poles can be connected to separate motor drive units in modular motors. These types of motors are also called split-winding motors [4], as the redundancy and fault tolerance of the system is enhanced thanks to this modularization. Moreover, the motor drive modules can be connected with different configurations which makes the design more flexible.

A general block diagram of one module of an IMMD system is shown in Fig. 2 [3]. On the machine pole, concentrated windings are preferred for their easy manufacturing and suitability for split-winding stators, especially in modular motors. Fractional slot concentrated winding (FSCW) permanent magnet synchronous motors (PMSMs) are very common in IMMD studies thanks to their high power density, high torque density, low cogging torque and good fault tolerance capability [6].

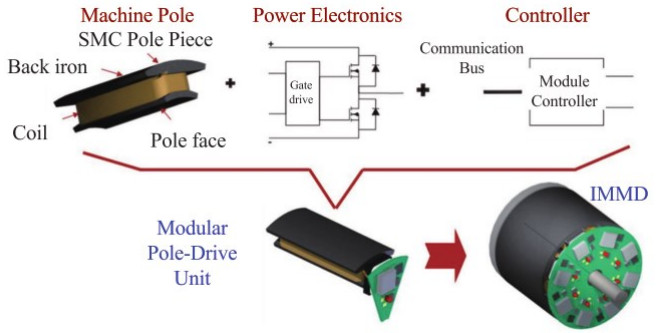

Fig. 2. General block diagram of one module of an IMMD [3]

As for the power electronics, many different topologies have been proposed for AC motor drive systems such as, two-level inverter, multilevel neutral point clamped inverter, multilayer flying capacitor inverter, inverter with high frequency transformer etc. [1]. As mentioned previously, for a modular motor drive, several other motor drive topologies become available thanks to the design flexibility. Furthermore, the aforementioned topologies can be connected in series and/or parallel on the DC link to form a new topology. Series and parallel connection of motor drive inverter modules on the DC link are shown in Fig. 3 alongside with a conventional motor drive [2]. These types of connections are possible due to the fact that the windings, which are split and hence electrically isolated, do not cause circulating currents among the inverter modules. The major advantage of this possibility is to be able to split the voltage and/or current requirement of each inverter. One practical usage of this fact is the availability of low voltage power semiconductor device utilization such as GaN in case of high DC link voltage.

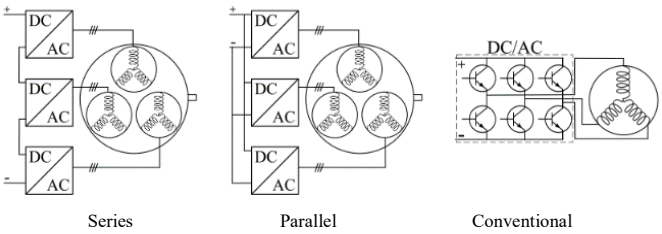

Fig. 3. Different motor drive inverter connections for a modular motor [2]

The employment of GaN devices is especially crucial for IMMD systems because these devices are one of the so-called WBG type semiconductor devices. These devices have much higher switching speeds compared to conventional silicon based devices such as Insulated Gate Bipolar Transistors (IGBTs) and admissible on-state losses which make them more efficient [7]. Moreover, they have higher maximum junction temperatures. The volume reduction challenge of IMMDs can be addressed by the utilization of GaNs thanks to higher efficiency which makes cooling easier, and their fast switching speed which enables high switching frequencies reducing the size of passive components. In high power applications, the maximum switching frequency which can be applied to an IGBT is limited to 20 kHz, whereas GaNs can be used with frequencies as high as 100 kHz in applications with kW range [7]. Another reason is that the efficiency of the system is high not only in rated power, but also for a wide range of output power [5]. As a matter of fact, GaNs have been utilized in most of the very first IMMD prototypes thanks to these reasons [3].

Selection of DC bus capacitor bank is very critical in IMMD systems in terms of power density since it usually constitutes 20% of the system volume and 30% of the system weight [1]. Moreover, the height of the motor drive is mostly determined by these capacitors. In conventional motor drive systems, usually aluminum electrolytic type capacitors are used thanks to its low cost and high capacitance per volume. However, they have low rms current rating per unit volume and they are not very reliable as they have relatively shorter lifetime which is highly dependent on the operating parameters [8]. On the other hand, metal film type capacitors are a better choice in terms of current ratings, lifetime and reliability. For these reasons, the most common capacitor type used in DC buses of IMMD systems is metal film. On the contrary to conventional motor drive applications, in addition to voltage, current and capacitance selection, power density, cost, height, thermal model and the effect of these parameters to the capacitor lifetime should be taken into account in IMMD systems.

III. Design of the IMMD System

The design process of the IMMD system can be considered in two-fold: design of the motor and design of the drive. The first assumption in the design process is that the motor drive input is a passive diode bridge rectifier with an LC DC link filter. The effects of this rectifier module on the rest of the system are kept out of the scope of this study. The machine is a three-phase

PMSM having a modular stator with FSCW. Considering the applications where IMMD concept is suitable, it is decided to design a low speed, high torque motor. The system parameters used in the design process are shown in Table 1.

The first parameters to be decided is the number of three-phase modules. As stated before, the number of series or parallel connected modules can be varied according to the voltage and current requirements and the system parameters such as the DC link voltage and total output power. It has also been specified that GaN transistors should be used to reach the efficiency ratings and meet the volume reduction challenge. Blocking voltage rating of the current commercial GaN transistors is 650V at most [7]. If two-level full-bridge motor drive inverter modules are used, the minimum power semiconductor blocking voltage rating in this design is 810V. This value is calculated based on a safety margin considering the voltage overshoot effects due to parasitic inductances and high switching speed. It is clear that, at least two series modules should be used with the aforementioned GaN devices. This also makes the total number of modules an even number.

TABLE I. THE SYSTEM PARAMETERS USED IN THE IMMD DESIGN PROCESS

DC link voltage, V_{dc}	540 V
Total output power, P_{out}	8 kW
Motor efficiency aim, $\eta_{m,a}$	93%
Drive efficiency aim, $\eta_{d,a}$	98%
Rated speed, N_r	600 rpm

There are various parameters which affect the number of parallel modules. One of them is the required power rating of each module which effect the current ratings of the semiconductor devices and drive efficiency. Another one is the number of stator slots. Instead of number of slots per pole per phase (q) that is used in conventional systems, a new parameter, number of slots per module per phase (w) is defined in IMMDs. For example, if two series and two parallel modules are used, the minimum number of slots that can be used is *24*. Finally, the effect of interleaving and its utilization for minimization of DC link capacitor bank size is considered to determine the number of modules. In [8], the effect of the number of modules and applied interleaving angle to the current ripple on the DC link capacitor bank is studied for an IMMD system, and it has been shown that selecting four modules yields best results in terms of DC link capacitor size. Using that result, it is decided to use a total number of *4 modules* which are connected in *2-series and 2-paralel* configuration. The schematic diagram of the suggested IMMD system topology is shown in Fig. 4.

A. Design of the Motor Parameters

The main dimensions of the motor are determined according to the torque requirement (T_m), magnetic loading (B) and electrical loading (A) selected for the IMMD application, as shown in (1). V stands for the volume which is shown in (2), where D_{is} is the bore diameter and L_a is the axial length of the motor. The aspect ratio, which is the ratio of the diameter to the length is selected as *1.0* for this application. The number of slots should be an integer multiple of 24 since the number of 3-phase modules is 4. For the given dimensions, 24 slots yield better results in terms of copper fill factor. Moreover, the number of rotor poles is found according to fundamental winding factor.

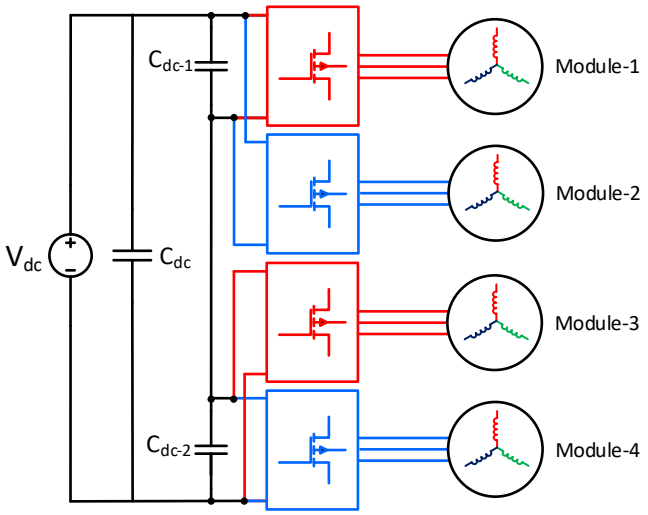

Fig. 4. Schematic diagram of the suggested IMMD topology

The number of turns per coil side can be determined by the induced voltage requirement of each phase of each module, which can be expressed as in (3), in *rms*, where $N_{ph\text{-}m}$ is number of turns per phase per module, f_s is the applied fundamental frequency at rated conditions, Φ_{pp} is the flux under a pole and k_w is the fundamental winding factor. The flux per pole can be calculated using the machine dimensions and air gap flux density (B_g) as in (4), where p is the number of poles. The winding factor is determined using the pre-calculated tables created for fractional slot machines in terms of slot/pole combinations as *0.933* [6]. The fundamental frequency is also determined by the rated speed and pole number of the synchronous motor, as in (5). Assuming that the motor drive inverters are switched with sinusoidal pulse width modulation (SPWM) technique, the terminal voltage of one phase of each module is determined using (6). The required number of turns per coil side, z_Q is found as *100* using (7).

The resultant motor parameters are shown in Table 2. In Fig. 5, the proposed 2-layer winding diagram of one module is shown. The main purpose behind the selection of this diagram is having large enough winding factor while keeping the harmonic content low.

$$T_m = V\ B\ A \tag{1}$$

$$V = \pi\ {D_{is}}^2\ L_a/4 \tag{2}$$

$$E_{ph-m} = 4.44\ N_{ph-m}\ f_s\ \Phi_{pp}\ k_w \tag{3}$$

$$\Phi_{pp} = 2\ D_{is}\ L_a\ B_g/p \tag{4}$$

$$f_s = N_m\ p\ /120 \tag{5}$$

$$V_{ph-m} = m_a\ V_{dc-m}/2\sqrt{2} \tag{6}$$

$$z_Q = 2\ N_{ph-m}/w\ l \tag{7}$$

TABLE II. THE RESULTANT MOTOR PARAMETERS

Number of stator slots, Q_s	24
Number of rotor poles, p	20
Motor axial length, L	150 mm
Stator outer diameter, D_{os}	210 mm
Stator inner diameter, D_{is}	155 mm
Air gap length, l_g	1 mm
Magnet thickness, l_m	3.5 mm
Number of turns per coil side, z_Q	100
Stator fill factor, k_{cu}	0.6
Stator winding factor, k_{ws}	0.933

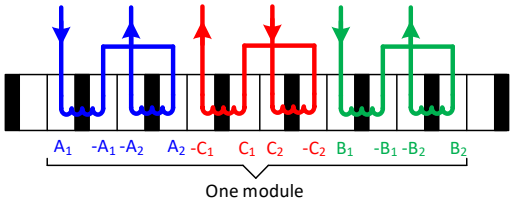

Fig. 5. Proposed winding diagram of one module

B. Design of the Drive

The selection of power semiconductor devices is based on voltage and current requirements. Among the suitable alternatives, the final selection is based on obtaining the highest motor drive efficiency. The voltage requirement of each device has already been established. There are two GaN transistor types in the market which have breakdown voltage ratings as high as 650V, cascade GaNs manufactured by Transphorm and enhancement mode (e-mode) GaNs manufactured by GaN Systems [7]. The next step is to determine the current requirement. By using the phase voltage calculated in the previous step, the phase current of each module can be found by using (8).

$$I_{ph-m} = P_{out-m} \,/\, [3\,\eta_m \cos(\varphi)\, f_s\, V_{ph-m}] \tag{8}$$

One device from each type is selected having similar ratings along with an IGBT for a better comparison, as shown in Table 3 [7]. Power semiconductor device losses can be categorized as forward conduction loss (P_{tc}), transistor switching loss (P_{ts}), reverse conduction loss (anti-parallel diode conduction loss for IGBTs, P_{dc}) and reverse recovery loss (P_{dr}). The analytical model used in the loss calculations is shown in (9) - (14). An approximate method which is well-established and commonly used for motor drive inverters is utilized for simplicity. In this model, I_{cp} and I_{ep} are the forward and reverse peak currents, respectively, f_{sw} is the switching frequency, φ is the power factor angle, E_{on} and E_{off} stand for turn-on and turn-off energies, $V_{ce\text{-}sat}$ is saturation voltage drop for the IGBT, $R_{ds\text{-}on}$ is the on-state resistance for GaN, V_{ec} is the reverse voltage drop, I_{rr} and t_{rr} are the diode reverse recovery current and time, respectively, and $V_{ce\text{-}p}$ is the reverse recovery peak voltage.

$$P_{tc} = I_{cp}\, V_{ce-sat}\, [1/8 + m_a \cos(\varphi)/3\,\pi] \quad (for\ IGBT) \tag{9}$$

$$P_{tc} = {I_{dp}}^2\, R_{ds-on}\, [1/8 + m_a \cos(\varphi)/3\,\pi] \quad (for\ GaN) \tag{10}$$

$$P_{ts} = \left(E_{on} + E_{off}\right) [f_{sw}/\pi] \tag{11}$$

$$P_{dc} = I_{ep}\, V_{ec}\, [1/8 - m_a \cos(\varphi)/3\,\pi] \quad (for\ IGBT) \tag{12}$$

$$P_{dc} = {I_{sp}}^2\, R_{ds-on}\, [1/8 - m_a \cos(\varphi)/3\,\pi] \quad (for\ GaN) \tag{13}$$

$$P_{dr} = I_{rr}\, t_{rr}\, V_{ce-p}\, [f_{sw}/8] \tag{14}$$

TABLE III. ALTERNATIVE DEVICES FOR TRANSISTOR SELECTION [7]

Device	**FP35R12KT4P**	**TPH3205WSB**	**GS66508B**
Type	IGBT	Cascode GaN	E-mode GaN
Manufacturer	Infineon	Transphorm	GaN systems
Voltage	1200 V	650 V	650 V
Current	35 A	35 A	30 A
$V_{ce,sat}$	2,15 V	-	-
$R_{ds,on}$	-	60 mΩ	50 mΩ

As mentioned previously, the selection of DC bus capacitor bank is very critical in IMMD systems due to power density constraints. In this paper, an optimum selection of DC link capacitors is performed for the designed system using metal film capacitors. For comparison, the same design procedure is also applied to the conventional system with IGBTs. The parameters affecting the capacitor selection are DC voltage (V_{dc}), capacitance requirement to meet the voltage ripple constraint (C_{dc}), the current requirement due to the rms rating of capacitor bank current ripple ($I_{c,rms}$) and temperature rise of each capacitor (T_c). The analytical model used for these parameters are shown in (15) - (18), where m_a is the modulation depth, $V_{dc\text{-}r}$ is the maximum allowed peak-to-peak voltage ripple, T_a is the ambient temperature, $R_{th\text{-}c}$ is the thermal resistance of the capacitor and R_c is the ESR value of the capacitors [8], [9].

$$C_{dc} = m_a \left(\widehat{I_s} - I_{avg}\right) / \left[2\, V_{dc-r}\, f_{sw}\right] \tag{15}$$

$$I_{c,rms} = I_{s,rms}\sqrt{\left[2\, m_a \left(\sqrt{3}/4\pi + \cos(\varphi)^2\left(\sqrt{3}/\pi - 9m_a/16\right)\right)\right]} \tag{16}$$

$$T_{core} = T_a + p_c(T_{core})\, R_{th,c} \tag{17}$$

$$p_c = {I_{c,rms}}^2\, R_c(T_{core}) \tag{18}$$

IV. SIMULATION RESULTS

The performance of the motor is analyzed using ANSYS/Maxwell simulation environment. The analytical results are shown in Table 4. The designed motor is simulated using 2D FEM analysis tool to obtain transient characteristics. The phase induced voltage, currents and machine torque are presented in Figs. 6, 7 and 8, respectively. The flux density distribution over one module is shown in Fig. 9. The efficiency of the motor is close to the targeted value, however the fill factor is made a little higher than the expected value to achieve this, which is still acceptable for concentrated windings. The 3rd order harmonic content of the induced voltage is actually cancelled on the line-to-line voltage thanks to the star connection. The torque ripple and cogging torque values are also below specified limits.

TABLE IV. MOTOR SIMULATION RESULTS (RMXPRT)

$E_{ph\text{-}m}$	71 V rms	J_{rms}	5.8 A/mm^2
$I_{ph\text{-}m}$	12 A rms	P_{cu}	411 W
T_m	127 Nm	P_{core}	117 W
k_{cu}	68 %	η_m	93.8 %

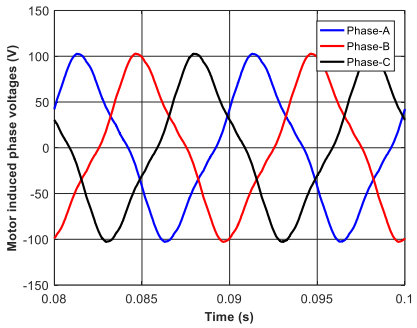

Figure 6. Induced phase voltages (2D FEM analysis)

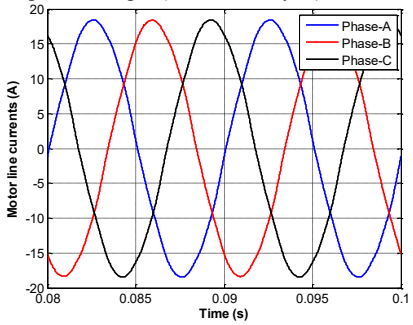

Figure 7. Line currents of one module (2D FEM analysis)

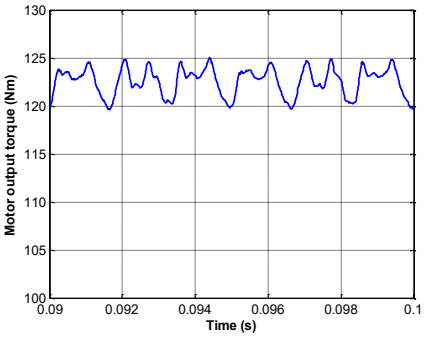

Figure 8. Motor output torque (2D FEM analysis)

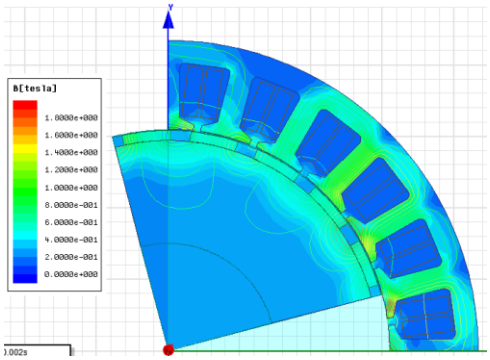

Figure 9. Flux density distribution over one module

Loss analysis for the drive is performed using the presented model, which includes the selected devices with a conventional system having IGBTs and two IMMD systems with different types of GaNs. The comparative loss results are shown in Figure 10. The results show that, even with a switching frequency five times the one with IGBTs, the total system loss is cut in half with GaN devices. The reason why 20 kHz is used for the system with IGBT is that, it is the practical limit for those devices. It is observed that the main reduction is on switching losses, as expected. However, transistor conduction losses are a little bit higher with GaNs, although reverse conduction losses are similar. There are two main reasons for this. First of all, IGBT conduction performance in high current applications is good. However, the GaN technology has not been proven itself in terms of on-state voltage drop, while it has developed to have comparable performance. Secondly, the IMMD system has 2-series structure so that each module carries two times the current they would have when there a 4 parallel modules. In conclusion, both cascade and e-mode GaN FETs reach 98% drive efficiency at 100 kHz switching frequency. Motor drive simulations are performed using 4 modules used with the proposed configuration, with 90^0 phase shift and suitable DC link capacitor which results in less than 1% voltage ripple. The DC link current is shown in Fig. 11, with and without interleaving. The DC link voltage ripple is also shown in Fig. 12.

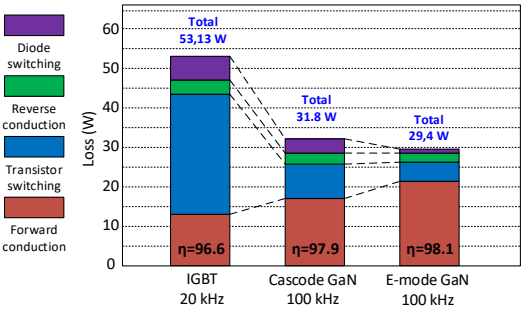

Figure 10. Comparative loss analysis having a conventional system with IGBT and two different IMMD systems with GaN

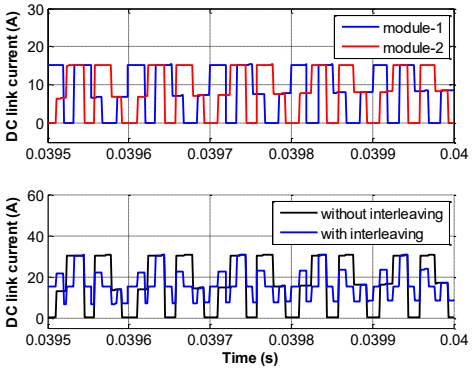

Figure 11. The DC link current of each module and total DC link current

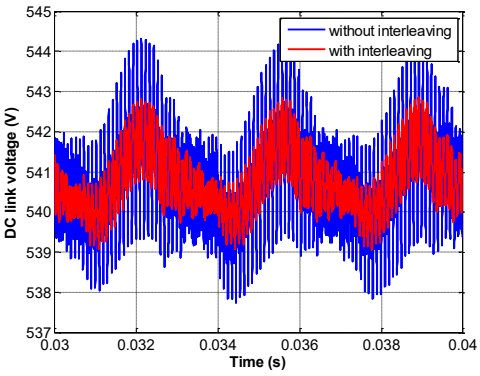

Figure 12. DC link voltage ripple with and without interleaving

The results show that, each module has an average DC link current of 8.23 A while rms ripple current of 6.93 A, which correspond to 77% of the average. With this IMMD configuration, the rms ripple current rating of each capacitor is 12.78 A without interleaving. When interleaving is applied with a phase shift of 90^0, which is the most suitable one for this case, the rms ripple current requirement drops to 6.69 A resulting in an improvement of 48%. Considering the voltage ripple constraint, 26 µF is required for each capacitor with 40 kHz switching frequency when interleaving is not applied. A similar improvement is also observed on capacitance requirement which drops to 14 µF when interleaving is applied. for the conventional system with IGBTs, the ripple current rating turns out to be 12.78 A and capacitance requirement is at least 100 µF at 10 kHz switching frequency. Of course, application of phase-shift with interleaving is not possible in this case.

Parameters of the capacitor bank (for only one of the series connected buses) design for the IMMD system are shown in Table 4. Using the thermal model, the temperature rise of the capacitors is verified to be less than 10 ^{0}C, which is acceptable although the ambient temperature is higher than a conventional system due to other heat sources in the environment like motor windings.

Finally, the resultant power density of both the capacitor bank and the overall system is analyzed to verify the performance of the design. Using the motor dimensions, PCB dimensions and capacitor heights, the power density of the capacitor bank and overall system are found as 35.27 W/cm^3 and 16.57 W/cm^3, respectively. This result shows that, the performance criteria defined for the design process have been achieved in terms of power density, efficiency and reliability.

TABLE IV. PARAMETERS OF THE CAPACITOR BANK

Capacitor	B32676G3306	**Connection**	2-parallel
Type	Metal Film	**Total Cap.**	60 µF
Capacitance	30 µF	**Voltage**	300 V
ESR	2.8 mΩ	**Current**	26 A
Dimensions	30x42 mm	**ESL**	12 nH
Thermal Res	10 ^{0}C/W	**Height**	45 mm

V. CONCLUSIONS

In this study, an integrated modular motor drive system is proposed which can replace conventional motor drive systems, and its design process is presented. The proposed system brings several advantages such as increased power density, enhanced fault tolerance and reliability, reduction in EMI problems and voltage stress across devices, and increased surface area for better cooling.

The design is based on 2-level inverter modules which can be connected in series and/or parallel on the DC link thanks to the modular structure. The number of series/parallel modules are established based on the reduction in the size of the DC link capacitor with proper interleaving angle, and the available device voltage and current ratings. Dimensioning of a PMSM having FSCW stator is performed and a suitable modular winding configuration is proposed. The design of the modular motor drive is based on WBG GaN power FETs selected from two different manufacturers. Loss characterization and analysis is performed using these devices along with a conventional converter in which IGBT is utilized for comparison.

It has been shown that both GaN devices yield superior efficiency performance even with a switching frequency five times the conventional one. Moreover, selection of DC bus capacitor banks is performed for these systems and the effects of interleaving, which is only applicable for modular structure, to the size of capacitors are presented. It is shown that, a power density as high as 15 W/cm^3 can be achieved with 98% motor drive efficiency for an IMMD. Considering also the improvements on the system reliability and fault tolerance, the performance of the IMMD system has been proven to be successful to replace the conventional motor drive systems using the design process presented here.

ACKNOWLEDGMENT

This work is partially supported by Scientific and Technological Research Council of Turkey (TUBITAK) under the TUBITAK project number 117E252.

REFERENCES

[1] G. Lo Calzo, G. Vakil, B. Mecrow, S. Lambert, T. Cox, C. Gerada, M. Johnson, and R. Abebe, “Integrated motor drives: state of the art and future trends,” *IET Electr. Power Appl.*, vol. 10, no. 8, pp. 757–771, Sep. 2016.

[2] M. D. Hennen, M. Niessen, C. Heyers, H. J. Brauer, and R. W. De Doncker, “Development and control of an integrated and distributed inverter for a fault tolerant five-phase switched reluctance traction drive,” *IEEE Trans. Power Electron.*, vol. 27, no. 2, pp. 547–554, 2012.

[3] J. Wang, Y. Li, and Y. Han, “Integrated Modular Motor Drive Design With GaN Power FETs,” *IEEE Trans. Ind. Appl.*, vol. 51, no. 4, pp. 3198–3207, 2015.

[4] J. J. Wolmarans, M. B. Gerber, H. Polinder, S. W. H. De Haan, J. A. Ferreira, and D. Clarenbach, “A 50kW integrated fault tolerant permanent magnet machine and motor drive,” *PESC Rec. - IEEE Annu. Power Electron. Spec. Conf.*, pp. 345–351, 2008.

[5] T. Morita, S. Tamura, Y. Anda, M. Ishida, Y. Uemoto, T. Ueda, T. Tanaka, and D. Ueda, “99.3% Efficiency of three-phase inverter for motor drive using GaN-based gate injection transistors,” *Conf. Proc. - IEEE Appl. Power Electron. Conf. Expo. - APEC*, pp. 481–484, 2011.

[6] S. U. Chung, J. M. Kim, D. H. Koo, B. C. Woo, D. K. Hong, and J. Y. Lee, “Fractional slot concentrated winding permanent magnet synchronous machine with consequent pole rotor for low speed direct drive,” *IEEE Trans. Magn.*, vol. 48, no. 11, pp. 2965–2968, 2012.

[7] E. A. Jones, F. F. Wang, and D. Costinett, “Review of Commercial GaN Power Devices and GaN-Based Converter Design Challenges,” *IEEE J. Emerg. Sel. Top. Power Electron.*, vol. 4, no. 3, pp. 707–719, 2016.

[8] M. Ugur and O. Keysan, “DC link capacitor optimization for integrated modular motor drives,” *2017 IEEE 26th Int. Symp. Ind. Electron.*, vol. i, pp. 263–270, 2017.

[9] J. W. Kolar and S. D. Round, “Analytical calculation of the RMS current stress on the DC-link capacitor of voltage-PWM converter systems,” *IEE Proc. - Electr. Power Appl.*, vol. 153, no. 4, p. 535, 2006.